Radiology

Imaging of Brown Adipose Tissue: State of the Art[1]

Srihari C. Sampath, MD, PhD, MPhil
Srinath C. Sampath, MD, PhD, MPhil
Miriam A. Bredella, MD
Aaron M. Cypess, MD, PhD
Martin Torriani, MD, MMSc

The rates of diabetes, obesity, and metabolic disease have reached epidemic proportions worldwide. In recent years there has been renewed interest in combating these diseases not only by modifying energy intake and lifestyle factors, but also by inducing endogenous energy expenditure. This approach has largely been stimulated by the recent recognition that brown adipose tissue (BAT)—long known to promote heat production and energy expenditure in infants and hibernating mammals—also exists in adult humans. This landmark finding relied on the use of clinical fluorine 18 fluorodeoxyglucose positron emission tomography/computed tomography, and imaging techniques continue to play a crucial and increasingly central role in understanding BAT physiology and function. Herein, the authors review the origins of BAT imaging, discuss current preclinical and clinical strategies for imaging BAT, and discuss imaging methods that will provide crucial insight into metabolic disease and how it may be treated by modulating BAT activity.

[1] From Musculoskeletal Biology and Bioimaging, Department of Pharmacology, Genomics Institute of the Novartis Research Foundation, San Diego, Calif (Srihari Sampath, Srinath Sampath); Division of Musculoskeletal Imaging and Intervention, Massachusetts General Hospital and Harvard Medical School, 55 Fruit St, Yawkey 6E, Boston, MA 02114 (M.B., M.T.); and Translational Physiology Section, Diabetes, Endocrinology, and Obesity Branch, National Institute of Diabetes and Digestive and Kidney Diseases, National Institutes of Health, Bethesda, Md (A.M.C.). Received February 15, 2015; revision requested March 31; revision received May 26; accepted May 4; final version accepted January 21, 2016. **Address correspondence to** M.T. (e-mail: mtorriani@mgh.harvard.edu).

Srihari C. Sampath and Srinath C. Sampath contributed equally to this work.

A.M.C. is an employee of the National Institutes of Health.

The past 5 years have seen unprecedented advances in the understanding of adipocyte physiology, with important insights into the metabolic contribution of brown adipocytes in adult mammals. The existence of brown adipose tissue (BAT) in eutherian (placental) mammals and human infants has long been known (1). Although cervical and supraclavicular areas of increased metabolism had been documented in the radiology literature (2), the recent explosion of interest in BAT metabolism is driven by the observation that metabolically active BAT can be observed with imaging in a significant fraction of the adult population (3–5). The existence of BAT in adult humans has led to substantial interest in the therapeutic potential of heat production by this tissue (thermogenesis) as a means to increase whole-body energy expenditure in obesity. Furthermore, the recent description that cold exposure can induce certain adipose cells toward a phenotype similar to BAT (6) has further broadened the implications of BAT metabolism for the treatment of obesity and insulin resistance. In light of the important role that BAT is thought to play in normal and pathologic energy expenditure, it is crucial that practicing radiologists understand the physiologic role of BAT and the evolving imaging methods to assess its presence and function.

Imaging-based approaches have been crucial for studying the presence and regulators of human BAT. Initial studies described an association between the presence of catecholamine-secreting tumors (pheochromocytoma) and brown fat tumors (hibernoma) (7), as well as the ability of pheochromocytomas to induce BAT overgrowth in remote sites (8), foreshadowing the now-well-known effect of cold and β3-adrenergic receptor signaling in activating BAT (9). However, the crucial observations regarding the presence of BAT in adults came with the advent of fluorine 18 (^{8}F) fluorodeoxyglucose (FDG) positron emission tomography (PET) and the identification of hypermetabolic activity in the cervical and supraclavicular regions (10). This was initially thought to reflect radiotracer uptake by muscle, but subsequent anatomic coregistration with ^{18}F FDG PET/computed tomography (CT) definitively established the existence of hypermetabolic fat in adults (2).

Although ^{18}F FDG PET/CT has clearly been useful in such proof-of-concept human studies, this approach has several important limitations, including heterogeneity of response, sensitivity to experimental or environmental factors, insensitivity to fatty acid–mediated metabolism (the preferred energy source for BAT), and confounding variables for standardized uptake value (SUV)–based quantitation (11). For these reasons, efforts are currently under way to develop alternative methods for BAT imaging, with the hope that this will allow noninvasive, quantitative measures of mass and activity. Current imaging approaches being investigated include alternative radionuclide-based approaches, advanced magnetic resonance (MR) imaging techniques, including spectroscopy and the use of hyperpolarized contrast media, and ultrasonographic (US) contrast agents.

Herein, we review the basic biology of BAT and the existing approaches used for imaging it, including techniques currently used in research applications as well as newer imaging approaches based on the expanding knowledge of the developmental origins and physiology of BAT. This review should provide the practicing radiologist with an understanding of the importance of BAT beyond confounding clinical ^{18}F-FDG imaging studies and will discuss how dedicated BAT imaging can contribute to the evaluation of metabolic disease.

Essentials

- Brown adipose tissue (BAT) regulates basal and inducible energy expenditure in humans and is composed of cells that contain numerous lipid droplets and mitochondria.
- BAT converts energy stores into heat by expressing uncoupling protein 1 (UCP1), which uncouples cellular respiration from energy production; clusters of UCP1-positive cells are also found amid white adipose tissue after cold exposure and are known as "beige" or "brite" adipocytes.
- Imaging of BAT has relied on its fluorine 18 (^{18}F) fluorodeoxyglucose (FDG) avidity, making ^{18}F FDG PET/CT the dominant modality for measuring its presence and quantity.
- Next-generation approaches for BAT imaging include specific PET tracers, MR imaging, and US-based strategies to determine BAT mass and activity.
- Imaging of BAT will be essential as investigators attempt to harness the biology of this tissue for the treatment of obesity, type 2 diabetes, and metabolic syndrome.

The Biology of BAT

Adipose tissue has been traditionally categorized as either white or brown, a distinction that reflects the histologic, anatomic, developmental, and functional differences between their respective adipocytic lineages (Fig 1) (12). From a bioenergetic standpoint, white adipose tissue (WAT) is primarily known for its role in energy storage in the form of unilocular triglyceride droplets, whereas brown adipocytes are highly specialized for heat production. This specialization is reflected by dense packing of mitochondria and multilocular intracellular lipid droplets,

Published online
10.1148/radiol.2016150390 **Content code:** MK

Radiology 2016; 280:4–19

Abbreviations:
BAT = brown adipose tissue
BOLD = blood oxygen level dependent
FDG = fluorodeoxyglucose
Glut-4 = glucose transporter protein 4
SUV = standardized uptake value
UCP1 = uncoupling protein 1
WAT = white adipose tissue

Conflicts of interest are listed at the end of this article.

Figure 1

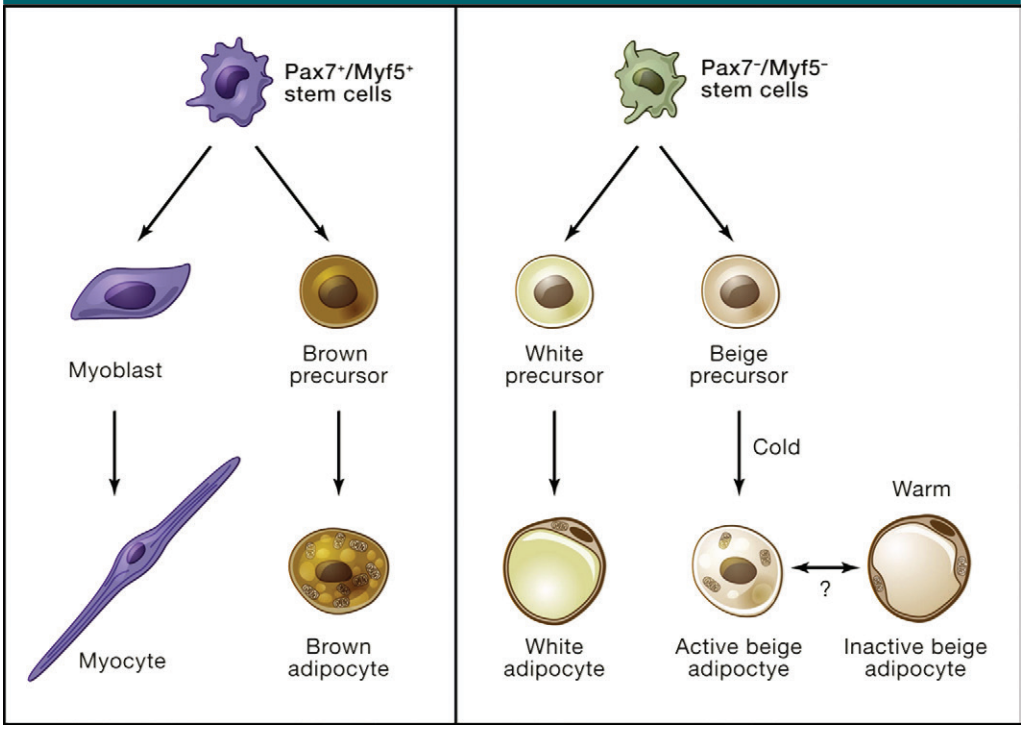

Figure 1: Distinct developmental origins of brown, white, and beige adipocytes. Unlike skeletal muscle and BAT, which arise from a common Pax7$^+$/Myf5$^+$ stem cell lineage (left), white and beige adipocytes appear to arise from Pax7$^-$/Myf5$^-$ cell lineage (right). (Reprinted, with permission, from reference 12.)

and crucially by expression of the mitochondria-associated uncoupling protein 1 (UCP1). UCP1 mediates biochemical uncoupling of electron transport by allowing proton leakage across the inner mitochondrial membrane, thus short-circuiting the usual linkage of electron transport to adenosine triphosphate production. Instead, the chemical energy generated by cellular respiration in brown adipocytes is dissipated in the form of heat, which allows thermoregulation by mammals in cold environments. It is estimated that fully activated BAT can produce up to 300 W/kg, whereas most other tissues produce only 1 W/kg (13).

Although the thermoregulatory function of BAT in small and hibernating mammals has been known for decades, the recent resurgence in interest on this tissue stems mainly from its potential to mitigate metabolic disease, specifically obesity and type 2 diabetes. Indeed, there is overwhelming evidence from genetic models demonstrating that increased amounts or activity of BAT can improve whole-body metabolism (12,14,15). The relevance of these observations was initially debated, given the limited amount of BAT in adult humans. However, the recent description of inducible "browning" of white fat has given new significance to these earlier studies (12).

It is now known that a certain population of UCP1-positive adipocytes within WAT can be induced to produce heat when stimulated by cold or peroxisome proliferator–activated receptor gamma agonists such as rosiglitazone (16,17). The developmental origin of this unique cell type, which has been termed "brite" (a portmanteau for "brown in white") fat, "beige" fat, or "induced WAT," appears to be distinct from that of classic BAT, which develops from a mesodermal population characterized by expression of muscle lineage markers *Myf5* and *Pax7* (18). Despite this distinct developmental origin, beige adipocytes express other BAT effector genes such as *Cidea* and *Pgc1a*, in addition to *Ucp1*. Likewise, it is clear that beige adipocytes can participate in thermogenesis (6).

Studies of WAT, BAT, and beige fat naturally led to the question of whether these pathways could be harnessed for metabolic benefit. Increased activity of BAT or beige fat leads to improvement in glucose tolerance and insulin sensitivity, and the observation that overexpression of *Pgc1a* was sufficient to convey many of these beneficial effects led to the identification of a cleaved version of the membrane protein FNDC5 as a potential mediator of browning and improved metabolism induced by exercise (19). Many other secreted inducers of browning have also been identified, including FGF21 (20,21), natriuretic peptides (22), and Bmp8b (23), which now represent attractive targets for drug development in obesity and diabetes (24). The development and application

of such targeted therapeutics will, however, require the establishment of imaging modalities to allow quantitative readout of thermogenic fat mass as well as activity (Table 1). In this review, "BAT imaging" refers to methods that reveal both classic BAT and beige cells, as current techniques are unable to help discriminate between these tissue types. Selective imaging of beige adipocytes is an important challenge that will be the subject of future investigations.

Prevalence of BAT in Humans

The prevalence of BAT in human subjects has been debated, with estimates derived from both retrospective and prospective studies (Table 2). Most retrospective studies have attempted to estimate BAT prevalence on the basis of analysis of PET/CT scans obtained under nonstandardized environmental and imaging conditions, an approach that allows large cohorts to be analyzed but has significant variability in degrees of BAT activation (40). Such studies have generally estimated the prevalence of active BAT to be approximately 5% (3,40), with variation in this percentage also attributable to differences in cohorts among studies.

In contrast, prospective studies of BAT prevalence generally use cold exposure to fully activate BAT metabolism, thus boosting the probability of detection. Such analyses have led to an estimated prevalence of 40%–100% in the general population (32,41,42). However, numerous factors have been described as contributing to the appearance of metabolically active (ie, ^{18}F-FDG–avid) BAT in humans. These include age (more frequently observed in younger subjects), sex (more frequent in women), and body mass index (less frequent in obese subjects) (3,25–27).

Imaging of BAT

PET Imaging

^{18}F-FDG PET/CT.—BAT imaging originated in the field of oncology imaging, specifically with use of ^{18}F-FDG PET/CT for the assessment of glucose uptake in tumors. FDG is a glucose analog that has selective uptake by glucose transporters (glucose transporter protein 1

Table 1

Current Approaches to BAT Imaging

Imaging Target and/or Mechanism	Imaging Modality	Advantages	Disadvantages
Glucose metabolism	^{18}F-FDG PET	Widely available, extensive clinical experience, depicts BAT activation	Ionizing radiation, limited anatomic information, glucose not preferred energy source for BAT, results dependent on imaging conditions and BAT activation level
Glucose metabolism with anatomic overlay	^{18}F-FDG PET/CT	Widely available, extensive clinical experience, depicts BAT activation, anatomic coregistration	Ionizing radiation, glucose not preferred energy source for BAT, results dependent on imaging conditions and BAT activation level, potential for misregistration
Membrane potential	^{18}F- or carbon 14 (^{14}C)-FBnTP PET	High accumulation in inactive BAT	Decreased signal after BAT activation
Sympathetic innervation	^{11}C-MRB PET	Preferential accumulation in BAT	Little increase in signal after BAT activation
Fatty acid uptake	^{18}F-THA PET	Activation-dependent uptake	Limited availability
Oxidative activity	^{11}C-acetate PET	Activation-dependent uptake	Limited availability, short half-life
Oxygen consumption	^{15}O-O_2 and ^{15}O-CO PET	Direct measurement of oxygen consumption, increased uptake with BAT activation	Limited availability, short half-life
Fat and/or water content	Chemical shift MR imaging	Noncontrast examination, widely available technique	Does not report on activation, limited for mixed BAT-WAT voxels
Fat and/or water proximity	Intermolecular zero-quantum coherence MR imaging	Allows BAT detection in mixed voxels, insensitivity to field inhomogeneity	Technically demanding, not yet validated in large patient cohorts
Activity-dependent blood flow	BOLD MR imaging	Clinically available, noncontrast examination, allows dynamic activation studies	Likely not useful for measuring BAT mass, not yet validated in large cohorts
Dynamic nuclear polarization	Hyperpolarized xenon 129 (^{129}Xe) or ^{13}C-MR imaging	Greatly enhanced signal-to-noise ratio, access to new substrates with which to probe BAT metabolism	Technically challenging, not widely available, short half-life of hyperpolarized substrates
Molecular and anatomic imaging	PET/MR imaging	Combines molecular imaging with tissue intrinsic contrast and anatomy	Not widely available, limited experience
Perfusion	Contrast-enhanced US	No ionizing radiation, lower cost, widely available, dynamic and/or serial examination possible	Limited to superficial BAT depots, no proof of principle in human subjects

Note.—BOLD = blood oxygenation level dependent, FBnTP = fluorobenzyl triphenyl phosphonium, MRB = (S,S)-O-methylreboxetine, THA = 14(R, S)-fluoro-6-thiaheptadecanoic acid.

Table 2

Factors That Affect the Prevalence of BAT in Human Retrospective Studies

Factor	Observed Effect on BAT Detection
Age	More frequent in younger patients (25–28)
Sex	More prevalent in women (25,26,28,29)
Ethnicity	No clear association (29–31)
Body mass index	Higher prevalence in subjects with normal body mass index, decreased or absent in severely obese subjects (25–29,32)
Basal metabolic rate	Positively correlated with basal metabolic rate (4,33)
Body fat content	Less prevalent in higher body fat content (4,32)
Anxiolytics	Decreased detection (34,35)
β-blocker usage	Decreased detection (36–38)
Outdoor temperature	Increased detection with lower average outdoor temperature (27,28)
Seasonal temperature	More frequently detected during winter months (32,39)

Note.—Future prospective studies with controlled BAT activation will provide more reliable insights into the true effect of the above factors, confirming those that in fact play a relevant role in the presence of human BAT.

or glucose transporter protein 4 [Glut-4]) and is trapped intracellularly by means of the action of hexokinase. It became apparent from early studies that "spurious" FDG uptake was often seen in areas with no discernible tumor, a finding usually attributed to muscle uptake in patients who were shivering. This represented a potential diagnostic dilemma until it was found that this uptake could be pharmacologically inhibited by means of pretreatment with benzodiazepines (eg, diazepam) or nonselective β-adrenergic blockers (eg, propranolol) (10,43). Separate studies demonstrated that this uptake often coincided with areas of low attenuation on coregistered CT scans, with Hounsfield unit measurements indicative of fat density (44). This was speculated to represent FDG uptake in BAT, which is consistent with earlier autopsy studies that indicated that BAT was both present and widely distributed in adult humans (1,2). Although these studies led to efforts in using ^{18}F-FDG PET/CT to estimate the prevalence and quantity of BAT, it was only in 2009 that a series of seminal articles definitively established that a specific pattern of cervical and upper thoracic FDG uptake in fact represented BAT (3–5,32,45). The years since the publication of these studies have seen an explosion of interest in the use of ^{18}F-FDG PET/CT to investigate the physiologic characteristics of BAT, being the dominant imaging modality used in the field.

It is important to appreciate the complex biology underlying ^{18}F-FDG uptake to properly evaluate studies by using ^{18}F-FDG PET/CT to investigate BAT function. Irrespective of tissue type, the overall cellular uptake of ^{18}F-FDG is dependent on two main factors: expression and activity of glucose transporters. Classic brown adipocytes demonstrate both high constitutive expression of Glut-4 as well as inducible expression of glucose transporter protein 1 and are therefore competent to uptake ^{18}F-FDG (46,47). Glut-4 is expressed in all insulin-sensitive tissues (skeletal muscle, heart, WAT, and BAT) and is under the control of complex regulatory mechanisms including insulin-dependent transporter translocation to the cell surface (48). In keeping with these findings, BAT demonstrates strong insulin sensitivity with regard to glucose uptake (49). In addition to insulin-dependent cell surface translocation, Glut-4 expression in BAT can also be directly regulated by other factors known to control BAT activation. This includes β-adrenergic signaling, which has been shown in animal studies to be required for cold-induced BAT activation and to increase expression of Glut-4 and UCP1 in BAT (50,51). Although both insulin and cold and/or β-adrenergic signaling promote ^{18}F-FDG uptake, they appear to do so by independent mechanisms, as cold (but not insulin) induces increased BAT perfusion that underlies its functions in energy dissipation and thermoregulation (49). Conversely, β-adrenergic signaling appears to be critically important not only for normal cold-induced activation of classic BAT, but also for the pathologic "browning" of white fat seen in cancer-induced cachexia (52). Finally, it is important to keep in mind that glucose is not the only or even the main energy source for BAT, which also demonstrates avid uptake of free fatty acids from the circulation (53).

The insulin sensitivity of BAT naturally makes ^{18}F-FDG PET/CT uptake critically dependent on many factors known to affect ^{18}F-FDG uptake in other tissues, such as skeletal muscle, heart, and tumors. This includes fasting status, diabetes, muscle activity, and medications such as β-blockers (3,25,27). As noted earlier, uptake is influenced by a host of patient-specific demographic and anthropometric factors, including age, sex, and body mass index (Table 2) (26,28,54). This makes proper and reproducible patient selection crucial in the assessment of the overall prevalence and distribution of BAT.

However, a most important factor is properly differentiating between presence and activity of BAT. Because ^{18}F-FDG is taken up primarily in active BAT, a lack of uptake can be due to either lack of BAT tissue or low levels of BAT activation. This dichotomy is clear from studies demonstrating large amounts of cold-activated BAT in patients who show no such BAT activation when exposed to warm conditions (55). This is in keeping with the observation that UCP1-positive brown adipocytes can be histologically identified in the supraclavicular fat regardless of ^{18}F-FDG uptake (56). Such effects may contribute to substantial intrasubject variability, an issue that has yet to be systematically addressed. Indeed, in a study of oncology patients undergoing serial ^{18}F-FDG PET/CT for tumor follow-up, less than 10% of patients with detectable BAT on an initial scan had

detectable BAT on a second study (25). Clearly, BAT activation status is both a complex and crucial factor for interpreting the results of ^{18}F-FDG PET/CT studies, especially those performed retrospectively.

In addition to complexities related to the mechanism of ^{18}F-FDG uptake in BAT, quantitating the results of these studies has proved to be challenging. This largely reflects a lack of standardization within the field as to how PET images are collected, cutoffs for SUVs to be considered positive for BAT, and CT attenuation criteria for separating fat from nonfat soft tissue. By convention, BAT is usually defined as metabolically active tissue (maximum SUV greater than a given threshold) localized to fat density (as determined with Hounsfield unit measurement) on coregistered CT scans. The threshold maximum SUV used in studies most commonly varies between 1.0 and 2.0, whereas Hounsfield unit cutoffs range from −10 to −250 (40). These two parameters can be cross-correlated to identify BAT on the basis of both its higher FDG uptake and its increased Hounsfield unit values compared with those of WAT, with the latter effect attributed to increased perfusion and higher intracellular water content (57,58). One potential use of such approaches is in automated segmentation of BAT from fused PET/CT images (59). Although promising, these efforts are currently limited by factors including the lower spatial resolution of PET in comparison with CT, misregistration of PET and CT images, and partial volume effects resulting in overestimation of BAT volume. Moreover, the specificity of CT in the detection of BAT remains to be determined.

Despite its methodologic limitations, ^{18}F-FDG PET/CT has proved to be an invaluable tool in BAT studies. Early studies focused on defining the prevalence and distribution of classic BAT, with widely varied results depending on experimental factors such as those discussed earlier. This has led to attempts to address this heterogeneity by studying more standardized populations (generally healthy, young, nonobese volunteers) in which BAT is also activated before imaging with a variety of cooling techniques. These studies have led to much higher estimates of the overall prevalence of detectable supraclavicular BAT, approaching 100% in studies in which tailored protocols are used to induce maximal activation, including cooling methods and β3-adrenergic receptor agonists (Figs 2–4; Table 3) (9,42,63). Beyond the classic supraclavicular depot, BAT uptake has also been demonstrated with ^{18}F-FDG PET/CT in a variety of additional sites, including cervical, mediastinal, upper thoracic, and paravertebral locations (3,40). Recent studies have also used ^{18}F-FDG PET/CT to investigate the relationship between BAT and a variety of pathologic states, including diabetes, obesity, human immunodeficiency virus lipodystrophy, bone loss, and cancer-associated cachexia (61,62,64,65). Among other findings, these studies have revealed an association of BAT mass and activity with bone mineral density, inhibited BAT activation in obesity, and an intermediate BAT phenotype in the dorsocervical fat of patients with human immunodeficiency virus lipodystrophy.

Going forward, ^{18}F-FDG PET/CT will undoubtedly continue to evolve and play a dominant role in BAT imaging. With regard to image acquisition, it is likely that further improvements in instrumentation will continue to deliver higher spatial resolution and decreased overall radiation doses. More sophisticated imaging protocols are likely to become prevalent, such as the use of dynamic rather than static PET imaging. This involves serial imaging beginning at the time of tracer administration and allows the calculation of glucose uptake rates and time-activity curves that are less sensitive to confounding factors that affect steady-state glucose metabolism (42,66). Beyond technical innovations related to image acquisition, the most impactful improvements for ^{18}F-FDG PET/CT may come in the realm of improved methods for standardized image quantitation and analysis. For instance, although current studies rely heavily on single-location maximum SUV as a readout of both BAT presence and activity, advances in automated segmentation will likely spur a movement toward the use of volumetric measurements such as mean SUV or total glycolytic activity (product of volume and mean SUV) as superior quantitative measures of BAT function (59).

Other PET/single photon emission CT tracers.—Although ^{18}F-FDG has proved to be the early workhorse of BAT imaging, a variety of other PET tracers have been investigated as sources of potentially valuable tissue contrast mechanisms. One of the earliest such tracers was ^{18}F- or ^{14}C-fluorobenzyltriphenyl phosphonium, a probe that accumulates in proportion to cellular membrane potential. Because mitochondria maintain an elevated membrane potential and are enriched in brown adipocytes, fluorobenzyltriphenyl phosphonium accumulates to high levels in inactive BAT (67). The downside of this approach is that tracer accumulation decreases in activated BAT, making it best suited for use as a marker of BAT volume rather than activity. This is also true for (S,S)-*O*-[^{11}C]methylreboxetine, a PET tracer that labels sites of sympathetic innervation by binding to the norepinephrine transporter. Although no published data are yet available regarding ^{11}C-methylreboxetine use in humans, preclinical data suggest that accumulation of this tracer is relatively high in inactive BAT (higher uptake relative to heart than for FDG); however, little increase is seen upon BAT activation (68).

Conversely, a substantial increase in uptake in activated BAT can be seen when using tracers responsive to nutrient uptake and metabolic status. Thus, both 14 (R,S)-[^{18}F]fluoro-6-thiaheptadecanoic acid (a marker of fatty acid uptake) and ^{11}C-acetate (a marker of oxidative activity) show increased uptake in BAT after activation in healthy human volunteers (69). Increases in activated BAT uptake have also been seen with ^{15}*O*-O_2 and ^{15}*O*-CO, both markers of oxygen consumption and, therefore, oxidative rate (60). In addition to fatty acid uptake and oxidative function, the crucial parameter of perfusion has also been

Figure 2

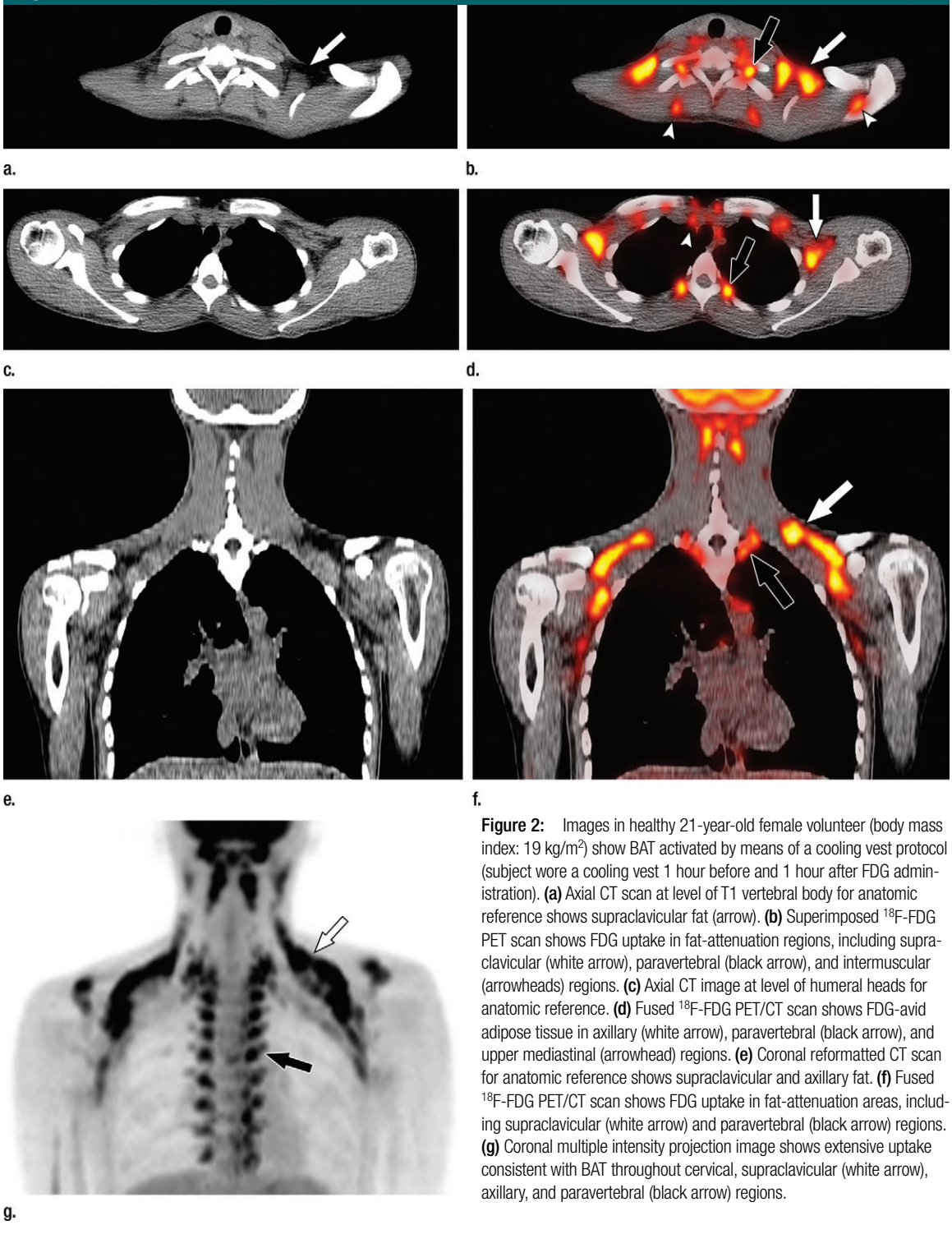

Figure 2: Images in healthy 21-year-old female volunteer (body mass index: 19 kg/m^2) show BAT activated by means of a cooling vest protocol (subject wore a cooling vest 1 hour before and 1 hour after FDG administration). **(a)** Axial CT scan at level of T1 vertebral body for anatomic reference shows supraclavicular fat (arrow). **(b)** Superimposed ^{18}F-FDG PET scan shows FDG uptake in fat-attenuation regions, including supraclavicular (white arrow), paravertebral (black arrow), and intermuscular (arrowheads) regions. **(c)** Axial CT image at level of humeral heads for anatomic reference. **(d)** Fused ^{18}F-FDG PET/CT scan shows FDG-avid adipose tissue in axillary (white arrow), paravertebral (black arrow), and upper mediastinal (arrowhead) regions. **(e)** Coronal reformatted CT scan for anatomic reference shows supraclavicular and axillary fat. **(f)** Fused ^{18}F-FDG PET/CT scan shows FDG uptake in fat-attenuation areas, including supraclavicular (white arrow) and paravertebral (black arrow) regions. **(g)** Coronal multiple intensity projection image shows extensive uptake consistent with BAT throughout cervical, supraclavicular (white arrow), axillary, and paravertebral (black arrow) regions.

Figure 3

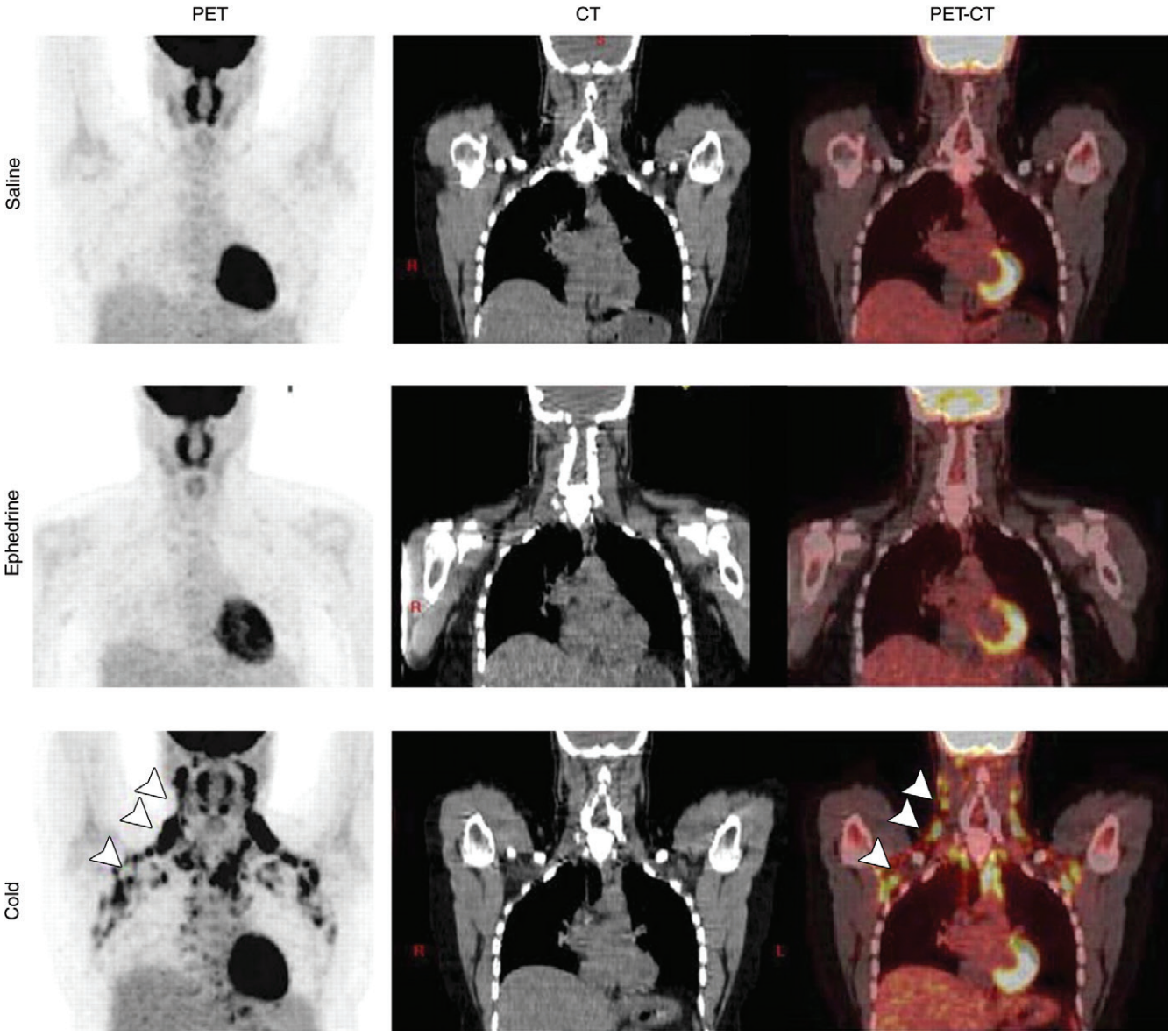

Figure 3: BAT activation induced by means of cold exposure but not sympathomimetic treatment. Coronal ^{18}F FDG PET (left column), CT (middle column), and fused PET/CT (right column) images in healthy volunteer after control saline treatment (top row), ephedrine treatment (middle row), or cold treatment by means of a cooling vest (bottom row). Arrowheads indicate tracer uptake specifically in response to cold treatment. (Reprinted, with permission, from reference 41.)

quantitated by using dynamic PET imaging with ^{15}O-H_2O (70). It should also be noted that BAT imaging with PET is not limited to small molecule approaches. New cell surface markers of brown adipocytes continue to be identified (71,72) and may be amenable to development as tracers by using immuno-PET approaches already validated for cell surface markers in other systems (73).

Finally, it should be noted that several other clinically used SPECT tracers, including technetium 99m (^{99m}Tc)-methoxyisobutylisonitrile (sestamibi) and iodine 123 (^{123}I)-metaiodobenzylguanidine, have been reported to depict BAT in both human and animal studies (74–76). Sestamibi is a perfusion agent that accumulates in cells with high cellular and mitochondrial membrane potentials, and the overall prevalence of detectable human BAT with use of ^{99m}Tc-sestamibi is approximately 6%–7%, which is similar to that observed in studies that used ^{18}F-FDG PET (77). Although increased

Figure 4

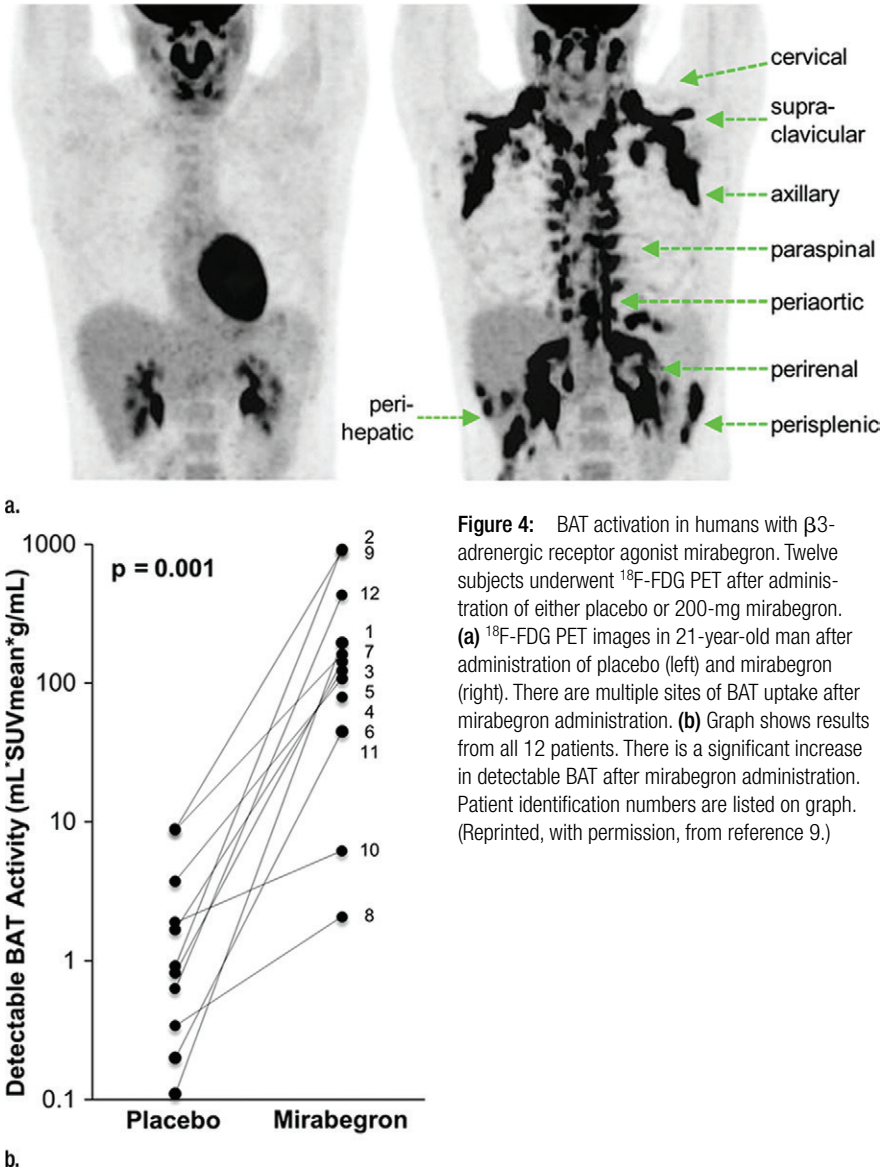

Figure 4: BAT activation in humans with β3-adrenergic receptor agonist mirabegron. Twelve subjects underwent ^{18}F-FDG PET after administration of either placebo or 200-mg mirabegron. **(a)** ^{18}F-FDG PET images in 21-year-old man after administration of placebo (left) and mirabegron (right). There are multiple sites of BAT uptake after mirabegron administration. **(b)** Graph shows results from all 12 patients. There is a significant increase in detectable BAT after mirabegron administration. Patient identification numbers are listed on graph. (Reprinted, with permission, from reference 9.)

uptake of ^{99m}Tc-sestamibi is seen in activated BAT, the change is small in comparison with PET agents such as ^{18}F-FDG (76), making it less suited for studies of BAT activity.

MR Imaging

The histologic differences between WAT and BAT create an opportunity to augment the signal obtained from BAT by virtue of its intrinsic contrast mechanisms. In particular, the multilocular lipid content, dense mitochondrial packing, and relatively higher capillarity within BAT collectively lead to significantly higher water content and increased magnetic susceptibility, raising the possibility of selective BAT imaging with use of MR imaging–based approaches. The lack of ionizing radiation makes MR imaging a particularly attractive modality, as it opens the door to repeated measurements in patients of all age groups.

One of the first MR imaging–based approaches attempted for BAT imaging used MR spectroscopy and chemical shift imaging. These techniques exploit the differential precession frequencies of protons between lipidic and aqueous environments to achieve water-fat separation (78). Early studies revealed that BAT could be successfully imaged by using this method, both ex vivo and in vivo (79,80). Subsequent studies further elucidated characteristic signatures of BAT by using MR spectroscopy, including lower levels of unsaturated triglycerides relative to WAT as well as expected lower fat and higher water fractions (Fig 5) (81). A related approach that used multiecho Dixon-based fat-water separation likewise demonstrated the possibility of separating BAT and WAT on the basis of relative fat fraction (82). In experimental animals, this approach successfully helped identify interscapular BAT and reduced BAT fat fraction with lower ambient temperature (82) and was subsequently used in human studies.

One limitation of the Dixon method is that it cannot be used to probe BAT content in mixed voxels; that is, situations where the voxel of interest contains both BAT and WAT could prevent quantification of lipid abundance. To overcome this limitation, a spectroscopy-based approach that uses intermolecular zero-quantum coherence transitions between lipid and water spins has been described (83). This approach relies on the fact that, as a consequence of smaller lipid droplet size, protons in water and lipids are in close proximity to one another within BAT, which therefore demonstrates maximal intermolecular zero-quantum coherence signal due to equal admixture of water- and fat-derived spins. The relevant spatial correlation scale of this technique is defined by the user and adjusted to the same order as the approximate diameter of an adipocyte. The authors demonstrate that this technique can be used to detect a water-methylene intermolecular zero-quantum coherence peak specific for BAT, and, as a result of the correlation length scale, the technique is intrinsically insensitive to field inhomogeneities

Table 3

Current Approaches to Activate Human BAT for ^{18}F-FDG PET/CT

Principle and Method	Comments
Adrenergic response by means of cold activation	
Temperature-controlled room (4)	Subject exposed to 16°C for 2 h, FDG administered after 1 h of cooling
Temperature-controlled room with lower extremity cooling (5,32)	Subject exposed to 19°C for 2 h, with legs intermittently on an ice block (for 4 min every 5 min); FDG administered after 1 h (27); 2 h at 17°–19°C with feet placed intermittently in ice water (5°–9°C; for 5 min every 10 min) (5)
Temperature-controlled room with fan cooling (60)	Subject exposed to approximately 2.5 h at 16°C with fan to provide low-level airflow; FDG administered after approximately1 h
Cooling vest (1,62)	Subject wears a vest with circulating chilled water at 5°C for 2 h (53); 2 h with cooling, the vest is set to 17°C (51); FDG administered after 1 h
Direct β3-adrenergic receptor agonism	
Preimaging treatment with mirabegron (9)	Temperature maintained at 23°C; 200-mg mirabegron given by mouth 3.5 h before FDG administration; imaging is performed 1 h later; treatment induces statistically significant increases in resting metabolic rate, heart rate, and systolic blood pressure

arising over larger scales. Further work from the same group demonstrated that this technique could be used in animals to generate BAT-specific coherence images, or BATSCI, which closely correlate with ^{18}F-FDG PET signal after BAT stimulation (84). The application of this approach in human subjects therefore represents an interesting avenue for further research.

Although spectroscopic and Dixon-based techniques clearly can help identify BAT-derived signal, these approaches are technically challenging, necessitating specialized pulse sequences and data analysis platforms. In principle, the simplest MR imaging–based approach for BAT imaging would use conventional (ie, clinically available) sequences. Recently, it was reported that BAT could be identified in small animals by using fast spin-echo sequences on the basis of the observation that signal intensity varied between BAT and WAT as a function of water content (85). With use of this approach, the authors demonstrated correlation with dissected BAT mass. Subsequently, the same group demonstrated that BAT could be detected in human subjects by using a water saturation approach that incorporates both T2-weighted spin-echo as well fast spin-echo sequences (86). This approach correlated well with the results of Dixon-based water-fat separation as well as with retrospective analysis of patient-matched ^{18}F-FDG PET/CT.

In addition to measuring BAT mass, MR imaging–based metrics and methodologies are also needed for quantifying the activity of BAT. The enriched vascular network within BAT raises the possibility that the increased cellular metabolism seen during activation might be accompanied by increased blood flow. This is known to be the case in the brain, where increase in activity-related blood flow has been extensively used in functional MR imaging by means of BOLD imaging, which exploits the differential paramagnetic properties of oxyhemoglobin and deoxyhemoglobin to generate contrast. In fact, BAT activation by the β3-adrenergic agonist CL-316,243 can be detected by using a functional MR imaging approach in small animals (85). To extend this work, the same group subsequently investigated whether BOLD signal changes could be observed with functional MR imaging in human subjects subjected to cold challenge. Volunteers were exposed to 13°–16°C for 60 minutes while wearing a vest circulating chilled water during MR imaging. In response to cold exposure, an increase in BOLD signal within BAT was noted, which was in fact substantially larger than that seen in the brain during conventional functional MR imaging (86) (Fig 6). This raises the possibility that BOLD-based MR techniques may have substantial utility for imaging BAT activation in dynamic studies.

Hyperpolarized MR imaging is another approach that may have utility in BAT imaging. Owing to the relatively low degree of polarization inducible by MR magnets, conventional MR imaging is limited to signal generated by proton spins in water or lipids. Hyperpolarized MR imaging uses in vitro nuclear spin polarization, providing orders of magnitude improvement in the signal-to-noise ratio, as well as access to new substrates as contrast agents (87). For instance, breakdown of hyperpolarized ^{13}C-pyruvate into bicarbonate and lactate was recently demonstrated in norepinephrine-activated interscapular BAT in rats (88). Noble gases in particular have been used as hyperpolarized contrast agents owing to their inert nature and, consequently, lower potential for biologic effects. An extensive literature now exists on pulmonary imaging with use of ^{129}Xe, which has proved to be a safe and effective tracer in humans (89). A recent study, moreover, reported the use of hyperpolarized ^{129}Xe gas to detect BAT activation, yielding a more than 15-fold increase in hyperpolarized xenon uptake within BAT during stimulation (90), which suggests that this approach represents a viable future approach for human BAT imaging. Intriguingly, use of the same agent to directly track BAT heat production by exploiting the temperature dependence of xenon chemical shift has been reported (90). The excitement surrounding hyperpolarized MR imaging must, however, be tempered by acknowledgment that this remains an experimental technique. Widespread

Figure 5

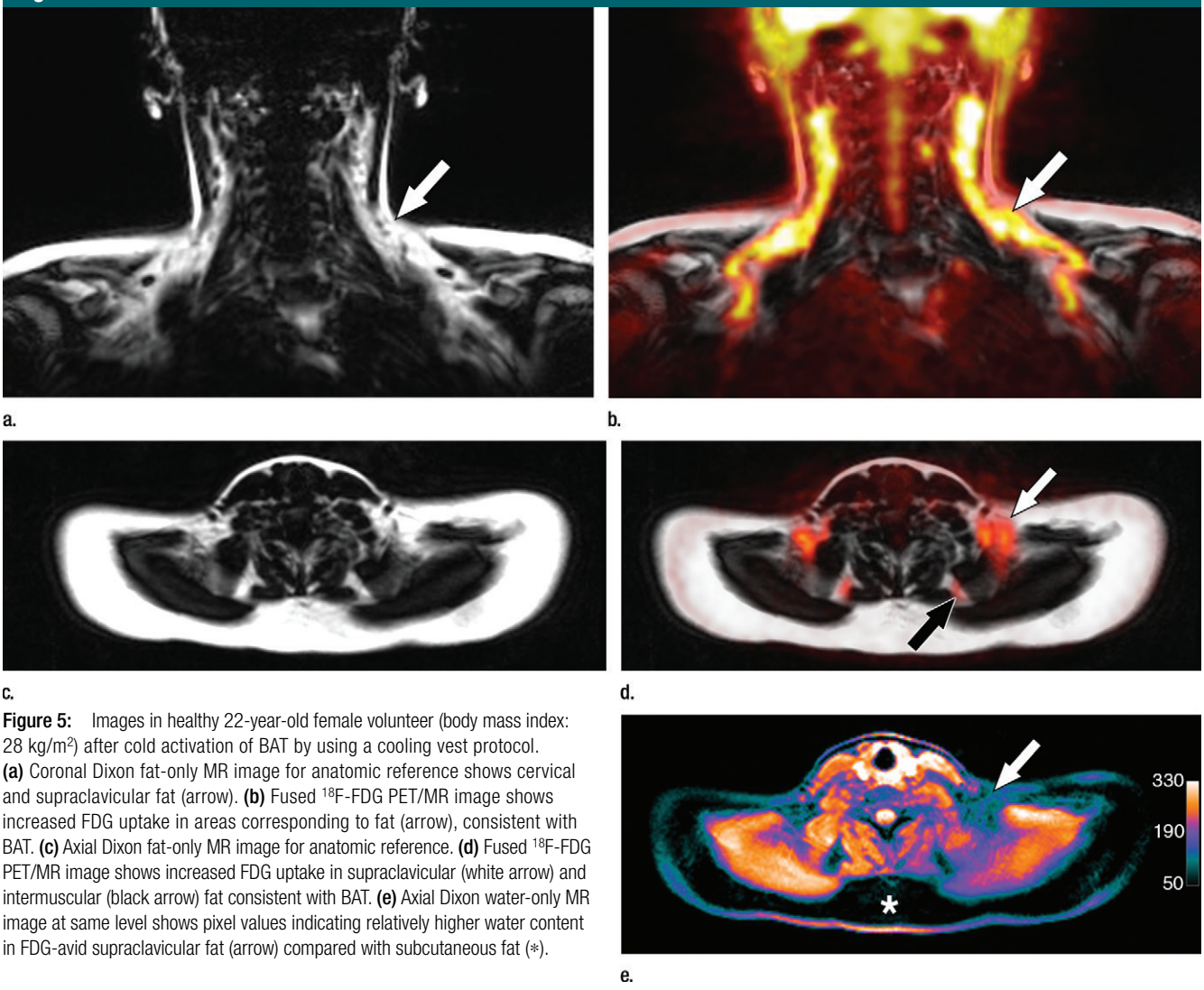

Figure 5: Images in healthy 22-year-old female volunteer (body mass index: 28 kg/m^2) after cold activation of BAT by using a cooling vest protocol. **(a)** Coronal Dixon fat-only MR image for anatomic reference shows cervical and supraclavicular fat (arrow). **(b)** Fused ^{18}F-FDG PET/MR image shows increased FDG uptake in areas corresponding to fat (arrow), consistent with BAT. **(c)** Axial Dixon fat-only MR image for anatomic reference. **(d)** Fused ^{18}F-FDG PET/MR image shows increased FDG uptake in supraclavicular (white arrow) and intermuscular (black arrow) fat consistent with BAT. **(e)** Axial Dixon water-only MR image at same level shows pixel values indicating relatively higher water content in FDG-avid supraclavicular fat (arrow) compared with subcutaneous fat (*).

adoption of hyperpolarized MR imaging will depend on the more general availability of hyperpolarizers and/or ready access to the polarized agents themselves, which generally have short half-lives.

As with most MR imaging–based approaches, the next generation of experimental implementations will almost certainly involve combined PET/MR imaging. The advantages of such an approach are obvious, as it captures both the molecular readout of PET with the sophisticated tissue-level analysis allowed by MR imaging (Fig 5). Indeed, there has already been an early stage report regarding the use of ^{18}F-FDG PET/MR imaging to detect BAT activation in response to either noradrenaline or adenosine A_{2A} receptor agonist treatment in mice (91). While this preclinical implementation appears promising, the true future promise of the technique lies in generating increasingly specific readouts of BAT mass and activation, both with PET and MR imaging. One can therefore imagine a future hybrid imaging modality that combines imaging of a BAT-specific cell surface receptor with PET to inform on mass with a BOLD MR imaging readout of activation.

US Imaging

Beyond PET and MR imaging, a variety of imaging techniques have shown promise for BAT imaging, most of which remain predominantly in the preclinical stage. The technique that seems best suited for clinical application is US. This is due to several key factors: it is relatively inexpensive, relies on widely available equipment and expertise, does not involve ionizing radiation, and can be used to dynamically interrogate numerous anatomic areas where BAT has been found. Because of these advantages, it also holds potential for serial imaging, a crucial point for

Figure 6

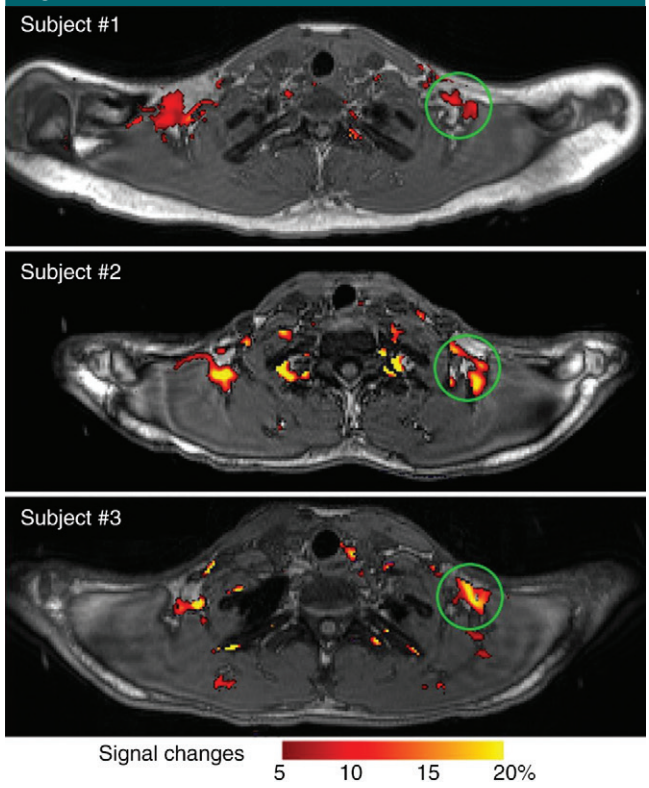

Figure 6: Detection of BAT activation in three human subjects with functional MR imaging. Significant BOLD signal changes (increasing from red to yellow) were detected after cold challenge (13°–16°C) and superimposed on anatomic images. Green circles indicate areas of cold-activated BOLD signal. (Reprinted, with permission, from reference 86.)

longitudinal studies involving pharmacologic interventions or natural history of disease. Although targeted tissue contrast techniques for US are still largely in the experimental stage, there is a large body of literature on the use of microbubbles for vascular contrast imaging (92). Early stage work in animals has indeed demonstrated the feasibility of microbubble contrast-enhanced US for BAT imaging (93). This approach uses brief pulses of high-energy ultrasound to locally destroy intravenously administered microbubbles, followed by dynamic imaging to monitor blood inflow (quantitated as reacquisition of microbubble-mediated contrast).

With use of this technique, BAT blood flow can be reliably quantitated and that flow increases after treatment with norepinephrine, which implies that BAT activation can be monitored noninvasively by using contrast-enhanced US (93). This is supported by the observation that a norepinephrine-induced increase in BAT perfusion was blunted in mice lacking UCP1, which also fails to induce oxygen consumption and thermogenesis in response to norepinephrine (94). In follow-up work, the same group demonstrated that total BAT mass could also be derived by using steady-state imaging during continuous norepinephrine and microbubble administration (95). Contrast-enhanced US–derived BAT mass correlated well with mass at necropsy, and the technique demonstrated reasonable intra- and interobserver variability. Overall, although this approach is limited to more superficial BAT depots owing to inherent technical limitations (eg, penetration depth), contrast-enhanced US is promising as a potentially clinically relevant technique allowing quantitation of both BAT volume and activation (Fig 7). This approach may become even more attractive if further advances in targeted US contrast eventually allow molecular targeting of contrast agents.

Other Imaging Modalities

Thermometry.—Another technique that has shown potential for clinical imaging is direct thermometry. Because the principal purpose of classic BAT is heat generation, it makes sense that heat measurement should be a direct reflection of BAT function. Indeed, studies in human subjects have demonstrated that thermal imaging can depict increases in supraclavicular temperature in response to cold challenge and that this increase is specific to the supraclavicular fossa (96,97). The ability to detect this increase is somewhat surprising given that most of the generated heat is likely to be dissipated to the circulation by means of BAT blood flow, and it remains to be seen if this will represent a challenge for further clinical applications. Although MR imaging can in principle be used to quantify thermogenic activity by using MR thermometry techniques, to our knowledge no studies have attempted BAT detection with this approach.

Preclinical techniques: near infrared fluorescence (peptide), fatty acid uptake, UCP1-luc.—Several optical approaches to BAT imaging have shown promise in animal models and, despite unclear translational potential, will doubtlessly have value in future preclinical studies. This includes optical imaging of ^{18}F-FDG itself by means of Cerenkov luminescence, demonstrating the expected accumulation in interscapular BAT (98). Other optical approaches include imaging of BAT vasculature by using a near-infrared coupled peptide probe, which allowed visualization of both inactive and activated interscapular BAT in animal studies (99). This probe notably also labeled subcutaneous beige fat, which has proved to be

Figure 7

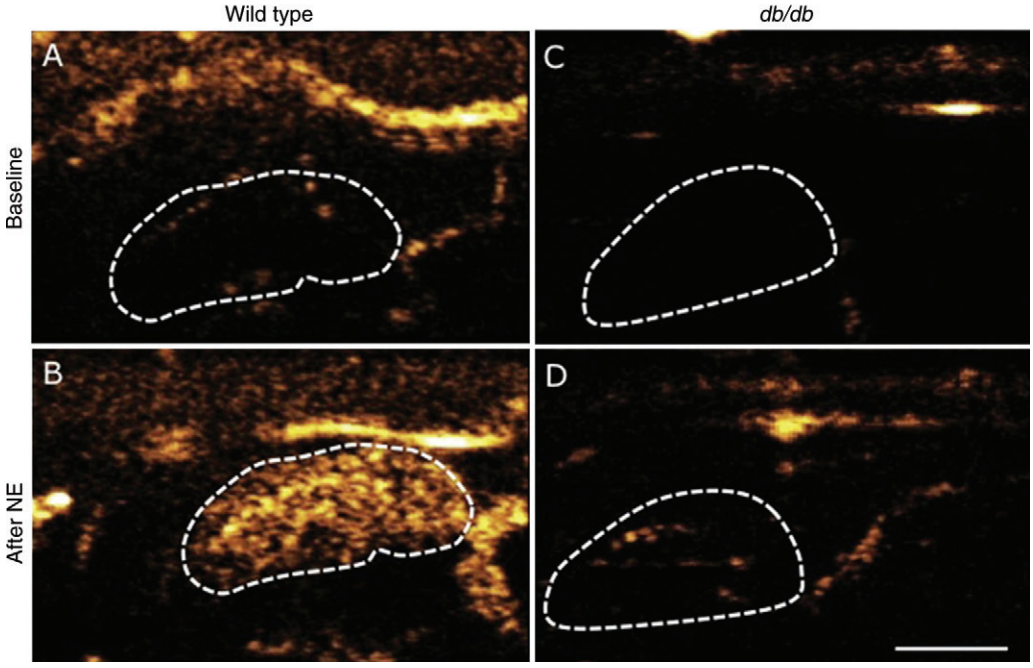

Figure 7: Contrast-enhanced US scans of, *A, B*, control or, *C, D*, obese *db/db* mice before (*A, C*) and after (*B, D*) intravenous infusion of BAT-activating factor norepinephrine (*NE*) show limited BAT activation in *db/db* mice. Dotted line indicates outline of left BAT lobe. White bar = 2.5 mm. (Reprinted, with permission, from reference 95.)

difficult with use of other techniques. Importantly, the conjugation chemistry that was used is compatible with radioisotope labeling and thus provides a way for clinical translation should this probe also prove specific in humans.

Finally, bioluminescence approaches have been used to image BAT and beige fat in transgenic mice. Covalent coupling of the luciferase substrate luciferin to an unbranched (62) fatty acid produced an imaging probe (FFA-SS-luc) that is specifically taken up in tissues that express fatty acid transporters, including skeletal muscle, heart, WAT, and BAT. BAT could then be imaged in transgenic mice expressing luciferase in all tissues (53). A more direct approach was taken in a recent study in which luciferase was placed under the direct control of the *UCP1* promoter, generating mice in which luciferase is expressed in all cells expressing *UCP1* (100). These animals proved useful for monitoring brown and beige fat with in vivo molecular imaging, as well as for generation of cell lines that can be used for screening to identify compounds capable of inducing UCP1 production.

Future Directions

The long-term goal in clinical BAT imaging is to develop noninvasive methods for detecting both BAT quantity and function with use of safe and clinically relevant techniques. Such approaches will further our understanding of the role of BAT in health and disease and also provide a prognostic marker of metabolic disease. Accomplishing this goal—in addition to selective imaging of beige fat—will require advances in BAT basic science (identification of specific and abundant markers), as well as in imaging sciences (improved PET standardization and quantitation, further exploration of MR imaging– and US-based methods, and selective BAT activation methods). Contributions will also likely come from better understanding the human genetic variation underlying differences in BAT abundance and activity. As with other diseases, the potential value of combining imaging and serum biomarkers should also be explored. Ultimately, the goal should be the development of a simple and noninvasive method for comprehensive BAT assessment that might provide an important biomarker of overall metabolic risk.

Conclusion

The obesity epidemic has made the development of new diagnostic and therapeutic approaches for metabolic disease an urgent priority. BAT imaging has the potential to contribute greatly in this regard and has made great strides from its origins in clinical nuclear medicine with ^{18}F-FDG PET. Although a wide variety of techniques are now available for both preclinical and clinical use, it is clear that each has limitations and none will individually suffice for all facets of BAT investigation. It is crucial that progress continues in each modality, which will

ensure that imaging techniques continue to play a central role in revealing the biology of BAT and its relevance for human metabolic disease.

Disclosures of Conflicts of Interest: Srihari C. Sampath Activities related to the present article: disclosed no relevant relationships. Activities not related to the present article: is an employee of the Genomics Institute of the Novartis Research Foundation, part of the Novartis Institutes for Biomedical Research. Other relationships: disclosed no relevant relationships. **Srinath C. Sampath** Activities related to the present article: disclosed no relevant relationships. Activities not related to the present article: is an employee of the Genomics Institute of the Novartis Research Foundation, part of the Novartis Institutes for Biomedical Research. Other relationships: disclosed no relevant relationships. **M.B.** disclosed no relevant relationships. **A.M.C.** Activities related to the present article: disclosed no relevant relationships. Activities not related to the present article: received grants from Chugai Pharma and Molecular Metabolism; received personal fees from Pfizer. Other relationships: disclosed no relevant relationships. **M.T.** disclosed no relevant relationships.

References

1. Heaton JM. The distribution of brown adipose tissue in the human. J Anat 1972;112(Pt 1):35–39.
2. Hany TF, Gharehpapagh E, Kamel EM, Buck A, Himms-Hagen J, von Schulthess GK. Brown adipose tissue: a factor to consider in symmetrical tracer uptake in the neck and upper chest region. Eur J Nucl Med Mol Imaging 2002;29(10):1393–1398.
3. Cypess AM, Lehman S, Williams G, et al. Identification and importance of brown adipose tissue in adult humans. N Engl J Med 2009;360(15):1509–1517.
4. van Marken Lichtenbelt WD, Vanhommerig JW, Smulders NM, et al. Cold-activated brown adipose tissue in healthy men. N Engl J Med 2009;360(15):1500–1508.
5. Virtanen KA, Lidell ME, Orava J, et al. Functional brown adipose tissue in healthy adults. N Engl J Med 2009;360(15):1518–1525.
6. Wu J, Boström P, Sparks LM, et al. Beige adipocytes are a distinct type of thermogenic fat cell in mouse and human. Cell 2012;150(2):366–376.
7. English JT, Patel SK, Flanagan MJ. Association of pheochromocytomas with brown fat tumors. Radiology 1973;107(2):279–281.
8. Dundamadappa SK, Shankar S, Danrad R, et al. Imaging of brown fat associated with adrenal pheochromocytoma. Acta Radiol 2007;48(4):468–472.
9. Cypess AM, Weiner LS, Roberts-Toler C, et al. Activation of human brown adipose tissue by a β3-adrenergic receptor agonist. Cell Metab 2015;21(1):33–38.
10. Barrington SF, Maisey MN. Skeletal muscle uptake of fluorine-18-FDG: effect of oral diazepam. J Nucl Med 1996;37(7):1127–1129.
11. Cypess AM, Haft CR, Laughlin MR, Hu HH. Brown fat in humans: consensus points and experimental guidelines. Cell Metab 2014;20(3):408–415.
12. Rosen ED, Spiegelman BM. What we talk about when we talk about fat. Cell 2014;156(1-2):20–44.
13. Symonds ME. Brown adipose tissue growth and development. Scientifica (Cairo) 2013;2013:305763.
14. Kopecky J, Clarke G, Enerbäck S, Spiegelman B, Kozak LP. Expression of the mitochondrial uncoupling protein gene from the aP2 gene promoter prevents genetic obesity. J Clin Invest 1995;96(6):2914–2923.
15. Stanford KI, Middelbeek RJ, Townsend KL, et al. Brown adipose tissue regulates glucose homeostasis and insulin sensitivity. J Clin Invest 2013;123(1):215–223.
16. Petrovic N, Walden TB, Shabalina IG, Timmons JA, Cannon B, Nedergaard J. Chronic peroxisome proliferator-activated receptor gamma (PPARgamma) activation of epididymally derived white adipocyte cultures reveals a population of thermogenically competent, UCP1-containing adipocytes molecularly distinct from classic brown adipocytes. J Biol Chem 2010;285(10):7153–7164.
17. Vitali A, Murano I, Zingaretti MC, Frontini A, Ricquier D, Cinti S. The adipose organ of obesity-prone C57BL/6J mice is composed of mixed white and brown adipocytes. J Lipid Res 2012;53(4):619–629.
18. Seale P, Bjork B, Yang W, et al. PRDM16 controls a brown fat/skeletal muscle switch. Nature 2008;454(7207):961–967.
19. Boström P, Wu J, Jedrychowski MP, et al. A PGC1-α-dependent myokine that drives brown-fat-like development of white fat and thermogenesis. Nature 2012;481(7382):463–468.
20. Coskun T, Bina HA, Schneider MA, et al. Fibroblast growth factor 21 corrects obesity in mice. Endocrinology 2008;149(12):6018–6027.
21. Fisher FM, Kleiner S, Douris N, et al. FGF21 regulates PGC-1α and browning of white adipose tissues in adaptive thermogenesis. Genes Dev 2012;26(3):271–281.
22. Bordicchia M, Liu D, Amri EZ, et al. Cardiac natriuretic peptides act via p38 MAPK to induce the brown fat thermogenic program in mouse and human adipocytes. J Clin Invest 2012;122(3):1022–1036.
23. Whittle AJ, Carobbio S, Martins L, et al. BMP8B increases brown adipose tissue thermogenesis through both central and peripheral actions. Cell 2012;149(4):871–885.
24. Schulz TJ, Tseng YH. Brown adipose tissue: development, metabolism and beyond. Biochem J 2013;453(2):167–178.
25. Lee P, Greenfield JR, Ho KK, Fulham MJ. A critical appraisal of the prevalence and metabolic significance of brown adipose tissue in adult humans. Am J Physiol Endocrinol Metab 2010;299(4):E601–E606.
26. Pfannenberg C, Werner MK, Ripkens S, et al. Impact of age on the relationships of brown adipose tissue with sex and adiposity in humans. Diabetes 2010;59(7):1789–1793.
27. Ouellet V, Routhier-Labadie A, Bellemare W, et al. Outdoor temperature, age, sex, body mass index, and diabetic status determine the prevalence, mass, and glucose-uptake activity of 18F-FDG–detected BAT in humans. J Clin Endocrinol Metab 2011;96(1):192–199.
28. Pace L, Nicolai E, D'Amico D, et al. Determinants of physiologic 18F-FDG uptake in brown adipose tissue in sequential PET/CT examinations. Mol Imaging Biol 2011;13(5):1029–1035.
29. Cronin CG, Prakash P, Daniels GH, et al. Brown fat at PET/CT: correlation with patient characteristics. Radiology 2012;263(3):836–842.
30. Perkins AC, Mshelia DS, Symonds ME, Sathekge M. Prevalence and pattern of brown adipose tissue distribution of 18F-FDG in patients undergoing PET-CT in a subtropical climatic zone. Nucl Med Commun 2013;34(2):168–174.
31. Admiraal WM, Verberne HJ, Karamat FA, Soeters MR, Hoekstra JB, Holleman F. Cold-induced activity of brown adipose tissue in young lean men of South-Asian and European origin. Diabetologia 2013;56(10):2231–2237.
32. Saito M, Okamatsu-Ogura Y, Matsushita M, et al. High incidence of metabolically active brown adipose tissue in healthy adult humans: effects of cold exposure and adiposity. Diabetes 2009;58(7):1526–1531.
33. Pasanisi F, Pace L, Fonti R, et al. Evidence of brown fat activity in constitutional leanness. J Clin Endocrinol Metab 2013;98(3):1214–1218.

34. Gelfand MJ, O'hara SM, Curtwright LA, Maclean JR. Pre-medication to block [(18)F]FDG uptake in the brown adipose tissue of pediatric and adolescent patients. Pediatr Radiol 2005;35(10):984–990.

35. Rakheja R, Ciarallo A, Alabed YZ, Hickeson M. Intravenous administration of diazepam significantly reduces brown fat activity on 18F-FDG PET/CT. Am J Nucl Med Mol Imaging 2011;1(1):29–35.

36. Söderlund V, Larsson SA, Jacobsson H. Reduction of FDG uptake in brown adipose tissue in clinical patients by a single dose of propranolol. Eur J Nucl Med Mol Imaging 2007;34(7):1018–1022.

37. Jacobsson H, Bruzelius M, Larsson SA. Reduction of FDG uptake in brown adipose tissue by propranolol. Eur J Nucl Med Mol Imaging 2005;32(9):1130.

38. Parysow O, Mollerach AM, Jager V, Racioppi S, San Roman J, Gerbaudo VH. Low-dose oral propranolol could reduce brown adipose tissue F-18 FDG uptake in patients undergoing PET scans. Clin Nucl Med 2007;32(5):351–357.

39. Zukotynski KA, Fahey FH, Laffin S, et al. Seasonal variation in the effect of constant ambient temperature of 24 degrees C in reducing FDG uptake by brown adipose tissue in children. Eur J Nucl Med Mol Imaging 2010;37(10):1854–1860.

40. Bauwens M, Wierts R, van Royen B, et al. Molecular imaging of brown adipose tissue in health and disease. Eur J Nucl Med Mol Imaging 2014;41(4):776–791.

41. Cypess AM, Chen YC, Sze C, et al. Cold but not sympathomimetics activates human brown adipose tissue in vivo. Proc Natl Acad Sci U S A 2012;109(25):10001–10005.

42. van der Lans AA, Wierts R, Vosselman MJ, Schrauwen P, Brans B, van Marken Lichtenbelt WD. Cold-activated brown adipose tissue in human adults: methodological issues. Am J Physiol Regul Integr Comp Physiol 2014;307(2):R103–R113.

43. Tatsumi M, Engles JM, Ishimori T, Nicely O, Cohade C, Wahl RL. Intense (18) F-FDG uptake in brown fat can be reduced pharmacologically. J Nucl Med 2004;45(7):1189–1193.

44. Cohade C, Osman M, Pannu HK, Wahl RL. Uptake in supraclavicular area fat ("USA-fat"): description on 18F-FDG PET/CT. J Nucl Med 2003;44(2):170–176.

45. Zingaretti MC, Crosta F, Vitali A, et al. The presence of UCP1 demonstrates that metabolically active adipose tissue in the neck of adult humans truly represents brown adipose tissue. FASEB J 2009;23(9):3113–3120.

46. Cannon B, Nedergaard J. Brown adipose tissue: function and physiological significance. Physiol Rev 2004;84(1):277–359.

47. Olsen JM, Sato M, Dallner OS, et al. Glucose uptake in brown fat cells is dependent on mTOR complex 2-promoted GLUT1 translocation. J Cell Biol 2014;207(3):365–374.

48. Richter EA, Hargreaves M. Exercise, GLUT4, and skeletal muscle glucose uptake. Physiol Rev 2013;93(3):993–1017.

49. Orava J, Nuutila P, Lidell ME, et al. Different metabolic responses of human brown adipose tissue to activation by cold and insulin. Cell Metab 2011;14(2):272–279.

50. Shimizu Y, Nikami H, Tsukazaki K, et al. Increased expression of glucose transporter GLUT-4 in brown adipose tissue of fasted rats after cold exposure. Am J Physiol 1993;264(6 Pt 1):E890–E895.

51. Tsukazaki K, Nikami H, Shimizu Y, Kawada T, Yoshida T, Saito M. Chronic administration of beta-adrenergic agonists can mimic the stimulative effect of cold exposure on protein synthesis in rat brown adipose tissue. J Biochem 1995;117(1):96–100.

52. Petruzzelli M, Schweiger M, Schreiber R, et al. A switch from white to brown fat increases energy expenditure in cancer-associated cachexia. Cell Metab 2014;20(3):433–447.

53. Henkin AH, Cohen AS, Dubikovskaya EA, et al. Real-time noninvasive imaging of fatty acid uptake in vivo. ACS Chem Biol 2012;7(11):1884–1891.

54. Yoneshiro T, Aita S, Matsushita M, et al. Brown adipose tissue, whole-body energy expenditure, and thermogenesis in healthy adult men. Obesity (Silver Spring) 2011;19(1):13–16.

55. Garcia CA, Van Nostrand D, Atkins F, et al. Reduction of brown fat 2-deoxy-2-[F-18] fluoro-D-glucose uptake by controlling environmental temperature prior to positron emission tomography scan. Mol Imaging Biol 2006;8(1):24–29.

56. Lee P, Zhao JT, Swarbrick MM, et al. High prevalence of brown adipose tissue in adult humans. J Clin Endocrinol Metab 2011;96(8):2450–2455.

57. Hu HH, Chung SA, Nayak KS, Jackson HA, Gilsanz V. Differential computed tomographic attenuation of metabolically active and inactive adipose tissues: preliminary findings. J Comput Assist Tomogr 2011;35(1):65–71.

58. Baba S, Jacene HA, Engles JM, Honda H, Wahl RL. CT Hounsfield units of brown adipose tissue increase with activation: preclinical and clinical studies. J Nucl Med 2010;51(2):246–250.

59. Ruth MR, Wellman T, Mercier G, Szabo T, Apovian CM. An automated algorithm to identify and quantify brown adipose tissue in human 18F-FDG-PET/CT scans. Obesity (Silver Spring) 2013;21(8):1554–1560.

60. Muzik O, Mangner TJ, Granneman JG. Assessment of oxidative metabolism in brown fat using PET imaging. Front Endocrinol (Lausanne) 2012;3:15.

61. Bredella MA, Fazeli PK, Freedman LM, et al. Young women with cold-activated brown adipose tissue have higher bone mineral density and lower Pref-1 than women without brown adipose tissue: a study in women with anorexia nervosa, women recovered from anorexia nervosa, and normal-weight women. J Clin Endocrinol Metab 2012;97(4):E584–E590.

62. Torriani M, Fitch K, Stavrou E, et al. Deiodinase 2 expression is increased in dorsocervical fat of patients with HIV-associated lipohypertrophy syndrome. J Clin Endocrinol Metab 2012;97(4):E602–E607.

63. van der Lans AA, Hoeks J, Brans B, et al. Cold acclimation recruits human brown fat and increases nonshivering thermogenesis. J Clin Invest 2013;123(8):3395–3403.

64. Bredella MA, Gill CM, Rosen CJ, Klibanski A, Torriani M. Positive effects of brown adipose tissue on femoral bone structure. Bone 2014;58:55–58.

65. Orava J, Nuutila P, Noponen T, et al. Blunted metabolic responses to cold and insulin stimulation in brown adipose tissue of obese humans. Obesity (Silver Spring) 2013;21(11):2279–2287.

66. Virtanen KA, Peltoniemi P, Marjamäki P, et al. Human adipose tissue glucose uptake determined using [(18)F]-fluoro-deoxy-glucose ([18F]FDG) and PET in combination with microdialysis. Diabetologia 2001;44(12):2171–2179.

67. Madar I, Isoda T, Finley P, Angle J, Wahl R. 18F-fluorobenzyl triphenyl phosphonium: a noninvasive sensor of brown adipose tissue thermogenesis. J Nucl Med 2011;52(5):808–814.

68. Lin SF, Fan X, Yeckel CW, et al. Ex vivo and in vivo evaluation of the norepinephrine transporter ligand [11C]MRB for

brown adipose tissue imaging. Nucl Med Biol 2012;39(7):1081–1086.

69. Ouellet V, Labbé SM, Blondin DP, et al. Brown adipose tissue oxidative metabolism contributes to energy expenditure during acute cold exposure in humans. J Clin Invest 2012;122(2):545–552.

70. Muzik O, Mangner TJ, Leonard WR, Kumar A, Janisse J, Granneman JG. 15O PET measurement of blood flow and oxygen consumption in cold-activated human brown fat. J Nucl Med 2013;54(4):523–531.

71. Wang W, Kissig M, Rajakumari S, et al. Ebf2 is a selective marker of brown and beige adipogenic precursor cells. Proc Natl Acad Sci U S A 2014;111(40):14466–14471.

72. Ussar S, Lee KY, Dankel SN, et al. ASC-1, PAT2, and P2RX5 are cell surface markers for white, beige, and brown adipocytes. Sci Transl Med 2014;6(247):247ra103.

73. Tavaré R, McCracken MN, Zettlitz KA, et al. Engineered antibody fragments for immuno-PET imaging of endogenous CD8+ T cells in vivo. Proc Natl Acad Sci U S A 2014;111(3):1108–1113.

74. Wong KK, Brown RK, Avram AM. Potential false positive Tc-99m sestamibi parathyroid study due to uptake in brown adipose tissue. Clin Nucl Med 2008;33(5):346–348.

75. Okuyama C, Sakane N, Yoshida T, et al. (123)I- or (125)I-metaiodobenzylguanidine visualization of brown adipose tissue. J Nucl Med 2002;43(9):1234–1240.

76. Cypess AM, Doyle AN, Sass CA, et al. Quantification of human and rodent brown adipose tissue function using 99mTc-methoxyisobutylisonitrile SPECT/CT and 18F-FDG PET/CT. J Nucl Med 2013;54(11):1896–1901.

77. Goetze S, Lavely WC, Ziessman HA, Wahl RL. Visualization of brown adipose tissue with 99mTc-methoxyisobutylisonitrile on SPECT/CT. J Nucl Med 2008;49(5):752–756.

78. Brateman L. Chemical shift imaging: a review. AJR Am J Roentgenol 1986;146(5):971–980.

79. Sbarbati A, Baldassarri AM, Zancanaro C, Boicelli A, Osculati F. In vivo morphometry and functional morphology of brown adipose tissue by magnetic resonance imaging. Anat Rec 1991;231(3):293–297.

80. Sbarbati A, Guerrini U, Marzola P, Asperio R, Osculati F. Chemical shift imaging at 4.7 tesla of brown adipose tissue. J Lipid Res 1997;38(2):343–347.

81. Hamilton G, Smith DL Jr, Bydder M, Nayak KS, Hu HH. MR properties of brown and white adipose tissues. J Magn Reson Imaging 2011;34(2):468–473.

82. Hu HH, Smith DL Jr, Nayak KS, Goran MI, Nagy TR. Identification of brown adipose tissue in mice with fat-water IDEAL-MRI. J Magn Reson Imaging 2010;31(5):1195–1202.

83. Branca RT, Warren WS. In vivo brown adipose tissue detection and characterization using water-lipid intermolecular zero-quantum coherences. Magn Reson Med 2011;65(2):313–319.

84. Branca RT, Zhang L, Warren WS, et al. In vivo noninvasive detection of brown adipose tissue through intermolecular zero-quantum MRI. PLoS One 2013;8(9):e74206.

85. Chen YI, Cypess AM, Sass CA, et al. Anatomical and functional assessment of brown adipose tissue by magnetic resonance imaging. Obesity (Silver Spring) 2012;20(7):1519–1526.

86. Chen YC, Cypess AM, Chen YC, et al. Measurement of human brown adipose tissue volume and activity using anatomic MR imaging and functional MR imaging. J Nucl Med 2013;54(9):1584–1587.

87. Couch MJ, Blasiak B, Tomanek B, et al. Hyperpolarized and inert gas MRI: the future. Mol Imaging Biol 2015;17(2):149–162.

88. Lau AZ, Chen AP, Gu Y, Ladouceur-Wodzak M, Nayak KS, Cunningham CH. Noninvasive identification and assessment of functional brown adipose tissue in rodents using hyperpolarized ^{13}C imaging. Int J Obes 2014;38(1):126–131.

89. Kirby M, Parraga G. Pulmonary functional imaging using hyperpolarized noble gas MRI: six years of start-up experience at a single site. Acad Radiol 2013;20(11):1344–1356.

90. Branca RT, He T, Zhang L, et al. Detection of brown adipose tissue and thermogenic activity in mice by hyperpolarized xenon MRI. Proc Natl Acad Sci U S A 2014;111(50):18001–18006.

91. Gnad T, Scheibler S, von Kügelgen I, et al. Adenosine activates brown adipose tissue and recruits beige adipocytes via A2A receptors. Nature 2014;516(7531):395–399.

92. Alzaraa A, Gravante G, Chung WY, et al. Targeted microbubbles in the experimental and clinical setting. Am J Surg 2012;204(3):355–366.

93. Baron DM, Clerte M, Brouckaert P, et al. In vivo noninvasive characterization of brown adipose tissue blood flow by contrast ultrasound in mice. Circ Cardiovasc Imaging 2012;5(5):652–659.

94. Matthias A, Ohlson KB, Fredriksson JM, Jacobsson A, Nedergaard J, Cannon B. Thermogenic responses in brown fat cells are fully UCP1-dependent. UCP2 or UCP3 do not substitute for UCP1 in adrenergically or fatty acid-induced thermogenesis. J Biol Chem 2000;275(33):25073–25081.

95. Clerte M, Baron DM, Brouckaert P, et al. Brown adipose tissue blood flow and mass in obesity: a contrast ultrasound study in mice. J Am Soc Echocardiogr 2013;26(12):1465–1473.

96. Symonds ME, Henderson K, Elvidge L, et al. Thermal imaging to assess age-related changes of skin temperature within the supraclavicular region co-locating with brown adipose tissue in healthy children. J Pediatr 2012;161(5):892–898.

97. Lee P, Ho KK, Lee P, Greenfield JR, Ho KK, Greenfield JR. Hot fat in a cool man: infrared thermography and brown adipose tissue. Diabetes Obes Metab 2011;13(1):92–93.

98. Zhang X, Kuo C, Moore A, Ran C. In vivo optical imaging of interscapular brown adipose tissue with (18)F-FDG via Cerenkov luminescence imaging. PLoS One 2013;8(4):e62007.

99. Azhdarinia A, Daquinag AC, Tseng C, et al. A peptide probe for targeted brown adipose tissue imaging. Nat Commun 2013;4:2472.

100. Galmozzi A, Sonne SB, Altshuler-Keylin S, et al. ThermoMouse: an in vivo model to identify modulators of UCP1 expression in brown adipose tissue. Cell Reports 2014;9(5):1584–1593.